Near-IR Photoresponse of Ruthenium Dipyrrinate Terpyridine Sensitizers in the Dye-Sensitized Solar Cells

Guocan Li,[†] Aswani Yella,[‡] Douglas G. Brown,[§] Serge I. Gorelsky,[#] Mohammad K. Nazeeruddin,[‡] Michael Grätzel,*,[‡] Curtis P. Berlinguette,*,[§] and Michael Shatruk*,[†]

[†]Department of Chemistry & Biochemistry, Florida State University, 95 Chieftan Way, Tallahassee, Florida 32306, United States

[‡]Laboratory for Photonics and Interfaces, Institute of Chemical Sciences and Engineering, School of Basic Sciences, Ecole Polytechnique Federale de Lausanne, Lausanne, Switzerland

[§]Departments of Chemistry and Chemical & Biological Engineering, The University of British Columbia, Vancouver, British Columbia V6T 1Z1, Canada

[#]Centre for Catalysis Research and Innovation, Department of Chemistry, University of Ottawa, Ottawa, Ontario K1N 6N5, Canada

S *Supporting Information*

ABSTRACT: Coordination of bidentate 5-pentafluorophenyldipyrrinate (pfpdp) or 5-(2-thienyl)dipyrrinate (2-tdp) to a Ru^{II} center bearing 2,2′:6′,2″-terpyridine-4,4′,4″-tricarboxylate (tctpy) and a NCS$^-$ ligand results in strongly light-absorbing complexes $[Ru(tctpy)(L)(NCS)]$ (L = pfpdp or 2-tdp). Anchored to a mesoporous TiO$_2$ electrode, these complexes afford a photoaction spectral response at wavelengths of up to 950 nm, one of the most red-shifted values reported to date for molecular dyes in the dye-sensitized solar cell (DSSC).

Dye-sensitized solar cells are a promising alternative to conventional (micro)crystalline silicon (c-Si) solar cells because of their relative ease of fabrication, environmental considerations, and high tolerance to impurities.[1] Nevertheless, c-Si solar cells still dominate the global photovoltaic market because, among other factors, the small band gap of silicon (1.1 eV) enables effective light-harvesting out to 1100 nm, while conventional DSSCs typically suffer from the poor collection of photons at $\lambda > 800$ nm. This scenario provides the impetus to develop sensitizers capable of more effectively capturing infrared (IR) light to increase the device efficiency.

While an efficient single-junction DSSC should convert all photons with $\lambda < 920$ nm (the threshold derived from the Shockley−Queisser equation[2]), very few dyes have been reported to provide long-wavelength light absorption.[3] The most prolific example is the so-called "black dye", $(Bu_4N)[Ru(tctpy)(NCS)_3]$ (**N749**),[4] which long stood as the most efficient DSSC sensitizer owing to the relatively broader spectral absorption of the complex. Nonetheless, the low-energy tail of the absorption band of **N749** suffers from a relatively low extinction coefficient, and thus moving the dominant metal-to-ligand charge-transfer (MLCT) band further into the IR region stands as a reasonable strategy for a higher current collection at $\lambda < 920$ nm. This goal has been realized through partial or complete substitution of the NCS$^-$ ligands of **N749** with chelating anionic cyclometalating and pyrazolate ligands among others.[5,6]

Dipyrrinate ligands have hitherto received far less attention in this context, which is somewhat surprising considering that their corresponding Ru(II) complexes are characterized by very high extinction coefficients. We previously demonstrated that appropriate consideration of the electronic properties of ruthenium dipyrrinato complexes containing polypyridyl anchoring ligands can render a dye motif capable of sensitizing TiO$_2$, but absorption for these dyes was limited to $\lambda < 750$ nm. Herein we report two new dyes, $[Ru(tctpy)(pfpdp)(NCS)]$ (**1**) and $[Ru(tctpy)(2-tdp)(NCS)]$ (**2**) (Figure 1), that differ in their
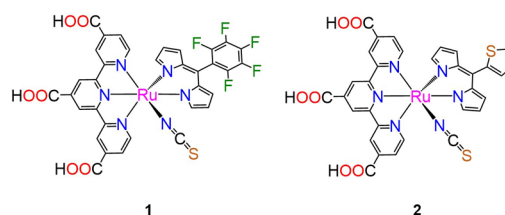

Figure 1. Molecular representations of **1** and **2**.

meso substituents on the dipyrrinates while maintaining charge distributions in the ground and excited states that are conducive to charge collection in the DSSC. Complexes **1** and **2** harvest light out to 950 nm, which is one of the lowest-energy photon-collection thresholds achieved with ruthenium sensitizers to date.

The synthesis of **1** involves reaction of the deprotonated dipyrrin with $[(p\text{-cymene})RuCl_2]_2$ to furnish $[(p\text{-cymene})Ru(pfpdp)Cl]$ (Scheme S1 in the Supporting Information). A subsequent halide abstraction with AgNO$_3$ in MeCN affords $[Ru(pfpdp)(MeCN)_4]NO_3$, which was successively treated with trimethyl-2,2′:6′,2″-terpyridine-4,4′,4″-tricarboxylate (Me$_3$tctpy) and KNCS to produce $[(Me_3tctpy)Ru(pfpdp)(NCS)]$ (**1a**). A facile hydrolysis step enables quantitative conversion of **1a** to **1**. The NCS$^-$ ligand can bind to ruthenium through either the nitrogen or sulfur atom, but the N-bound species is typically the thermodynamically favorable isomer for Ru(II) complexes. The NMR spectrum of **1a** indicated exclusive formation of the N-bound isomer (Figure S1 in the Supporting Information, SI), but ∼16% of the S-bound isomer was present in

the case of **1**, which was confirmed by the IR spectrum of **1** (Figure S2 in the SI). Complex **2** was synthesized following a similar protocol, also yielding the N- and S-bound linkage isomers in a 10:1 ratio.

The absorption spectra of **1** and **2** in MeCN are congruent (Figure 2). The negligible influence of the meso substituent on
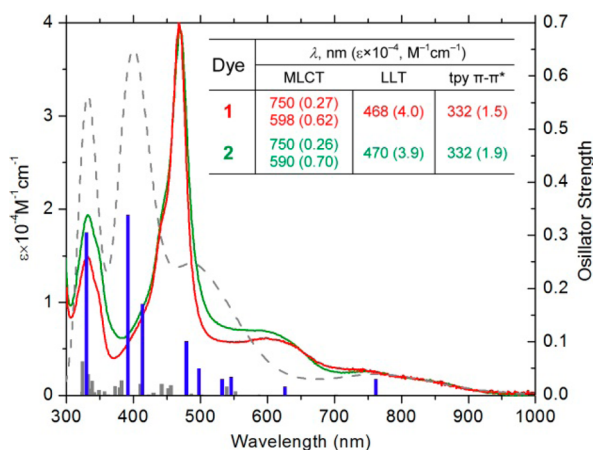
Figure 2. Experimental absorption spectra of **1** (red) and **2** (green) and the calculated spectrum of **1** (dotted gray) in MeCN at room temperature. The oscillator strengths of calculated transitions are shown as gray vertical lines with the major transitions highlighted in blue.

the optical properties is rationalized by the limited conjugation between the substituent and the dipyrrinato moiety because of the lack of coplanarity. The strong absorption band at 470 nm ($\varepsilon \sim 40000$ M^{-1} cm^{-1}) considerably improves the absorptivity of **1** and **2** in the visible region compared to that of **N749**.[4] A moderate band at ~600 nm is attributed to the MLCT transition from the ruthenium ion to the tctpy ligand. The MLCT band has a distinctive shoulder at ~750 nm, a feature not observed for **N749**. The low-energy extension of this shoulder provides substantial absorption of **1** and **2** in the IR region, with an onset at ~950 nm (Figure S3 in the SI). Emission was not detected for **1** at room temperature, consistent with our observations for other Ru(II) dipyrrinates,[8] but a prominent emission signal centered at 870 nm was observed at 77 K in an EtOH/MeOH glass [4:1 (v/v); Figure S4 in the SI].

To assign the absorption bands to specific electronic transitions, density functional theory (DFT)/time-dependent DFT calculations were performed on **1** and **2** using the implicit solvent model for MeCN (Table S1 in the SI). The highest occupied molecular orbital (HOMO) for both complexes contains contributions from the Ru 4d orbital (46%) and the NCS^- π orbital (31−33%), which is consistent with other NCS-containing Ru sensitizers.[9] This metal−ligand orbital mixing ostensibly benefits dye regeneration because the oxidized dye will have a substantial amount of hole density on the NCS^- ligand to better interact with the redox mediator in the electrolyte.[10] The HOMO−1 of **1** is also a mixed Ru-NCS orbital, while the HOMO−2 is mainly located on the dipyrrinate (Figure 3). The order of these two orbitals is reversed in the case of **2** because the electron-donating nature of the meso substituent destabilizes the dipyrrinato-based π orbital. The energies of the dipyrrinato-based orbitals in **1** and **2** are, nonetheless, similar, highlighting the limited conjugation between the meso substituent and the dipyrrinato fragment (Figure S5 in the SI). The lowest unoccupied molecular orbitals (LUMOs) are not affected
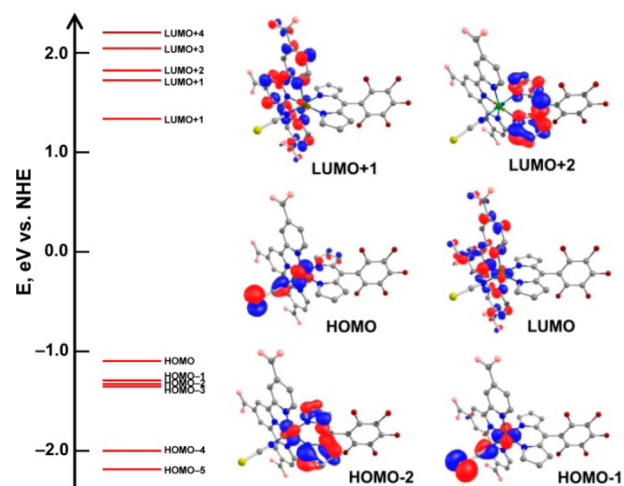
Figure 3. Selected frontier molecular orbitals of **1**. Isosurface contour values are 0.05 au. Hydrogen atoms are omitted for clarity. Color scheme: Ru, green; S, yellow; O, pink; N, blue; C, gray; F, maroon.

significantly by the meso substituent, and thus their character is similar in both **1** and **2**; namely, LUMO, LUMO+1, and LUMO+3 are localized on the tctpy π* orbitals and LUMO+2 is localized on the dipyrrinato π* orbital. In both cases, the tctpy-based LUMO is extended onto the carboxylic groups and well separated in energy from the higher-lying molecular orbitals, which provides the well-defined lowest excited state with strong electronic coupling to the TiO_2 acceptor states.

The simulated optical absorption spectrum of **1** reproduces the main features of the experimental spectrum (Figure 2 and Table S2 in the SI). The absorption band at 470 nm corresponds to the pfpdp $\pi \to \pi$* and interligand $\pi \to \pi$* (pfpdp $\to$ tctpy) transitions with a nominal MLCT contribution. The lower-energy band at ~600 nm is mainly of MLCT (Ru $\to$ tctpy) character. The shoulder at 700−800 nm is due to the HOMO $\to$ LUMO MLCT excitation process. The absorption bands of **2** are similar in nature; the complete excitation assignments are provided in Figure S6 and Table S3 in the SI.

Cyclic voltammograms were recorded on **1** and **2** in a MeCN solution using $(Bu_4N)PF_6$ as the supporting electrolyte at a scan rate of 0.1 V s^{-1}. The complexes exhibit a reversible oxidation wave centered at 0.93 and 0.88 V vs NHE, respectively (Figure S7 in the SI). Analysis of the DFT-calculated spin-density distributions for 1^+ and 2^+ (Figure S8 in the SI) indicates that the electron is removed from the HOMO of the neutral complexes upon oxidation. The DFT-optimized structures of 1^+ and 2^+ feature the Ru atom with a spin density of 0.62. The NCS^- ligand contributes 0.24 and 0.21 to the spin density in 1^+ and 2^+, respectively. The oxidation of **2** is cathodically shifted by 0.05 V relative to **1** (corroborated by a 0.06 V shift modeled by DFT) because of the more electron-donating 2-thienyl substituent in **2**.

The excited-state reduction potential, $E_{S^+/S*}$, was estimated from $E_{S^+/S*} = E_{S^+/S} - E_{0-0}$, where $E_{S^+/S}$ is the Ru(III) reduction potential and E_{0-0} was determined by the intersection of the absorption and normalized emission spectra (Figure S4 in the SI). This procedure led to $E_{S^+/S*} = -0.56$ and -0.61 V for **1** and **2**, respectively, and confirmed that the lowest excited state is positioned above the TiO_2 conduction band edge (-0.5 V vs NHE). The $E_{S^+/S}$ values for **1** and **2** are also lower than the reduction potential for the $I_2^{\bullet-}/I^-$ couple ($+0.8$ V),[11] and thus both the ground and excited states of **1** and **2** are positioned

appropriately for use in a conventional DSSC-containing TiO_2 electrode and iodide-based electrolytes.

The dyes were evaluated in the DSSC under AM 1.5 conditions using cells constructed with an electrode containing a 12-μm active layer of TiO_2 and a 3-μm scattering overlayer of TiO_2. The electrolyte contained 0.7 M LiI and 0.06 M I_2 in MeCN/valeronitrile (85:15, v/v) with 0.1 M guanidinium thiocyanate and 0.3 M 1,3-dimethylimidazolium iodide as additives. The incident photon-to-current efficiency (IPCE) curve (Figure 4)
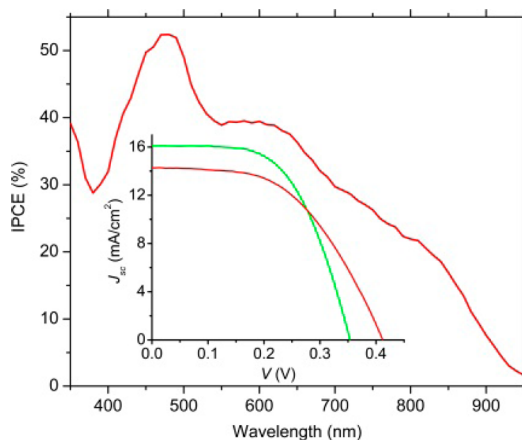
Figure 4. IPCE curve of **1**. Inset: photocurrent density−voltage (*I*−*V*) curve of DSSCs prepared with dyes **1** (red) and **2** (green) and recorded under AM1.5 illumination.

tracks the optical absorption spectrum and reaches a maximum value of 54% at 480 nm. The IPCE maintains a lower value of 40% over the 550−650 nm range and decreases gradually at progressively longer wavelengths. The onset of the IPCE curve is at 950 nm, which is one of the highest IPCE onset values for any reported ruthenium sensitizer.

Current−voltage (*I*−*V*) measurements of **1** (Figure 4, inset) revealed a modest power conversion efficiency (PCE) of 3.06% due to a low open-circuit voltage (V_{oc}) of 0.41 V and a fill factor of 51%, but a high current density (J_{sc}) was retained (14.35 mA cm^{-2}). Under similar conditions, **2** yielded a PCE of 3.27%, with J_{sc}, V_{oc}, and a fill factor of 16.11 mA cm^{-2}, 0.35 V, and 0.57, respectively. The higher J_{sc} value of dye **2** compared to that of dye **1** is consistent with the more negative excited-state oxidation potential of **2**. The decrease in V_{oc} is due to destabilization of the HOMO level of **2** relative to **1**. Our efforts to improve the V_{oc} value using *tert*-butylpyridine in the DSSC electrolyte[10] compromised the current to a significant extent, indicating that the positions of the excited states are at the threshold for injection.[8] Despite this setback, both V_{oc} and J_{sc} were significantly improved relative to $[Ru(H_2dcbpy)(Hdcbpy)_2(2\text{-}tdp)]$ (dcbpy = 2,2′-bipyridine-4,4′-dicarboxylate) documented in an earlier report.[7b] It appears that the NCS$^-$ groups play a critical role in improving the dye performance by acting as a better site for dye regeneration than the pyridyl ligand. Future studies will seek to elucidate this effect.[13]

In summary, two novel heteroleptic ruthenium(II) complexes bearing a dipyrrinato ligand that differs in the meso substituent have afforded substantially improved optical absorptivities in the visible and IR regions. The IPCE curves for **1** and **2** show sensitization out to 950 nm, a rare observation for ruthenium dyes, which points to the possibility of developing efficient near-IR sensitizers relying on ruthenium dipyrrinates.

■ ASSOCIATED CONTENT

Ⓢ Supporting Information

Synthesis, additional spectra and voltammograms, and results of DFT calculations on **1** and **2**. This material is available free of charge via the Internet at http://pubs.acs.org.

■ AUTHOR INFORMATION

Corresponding Authors

*E-mail: michael.graetzel@epfl.ch.
*E-mail: cberling@chem.ubc.ca.
*E-mail: shatruk@chem.fsu.edu.

Notes

The authors declare no competing financial interest.

■ ACKNOWLEDGMENTS

■ REFERENCES

(1) Hagfeldt, A.; Boschloo, G.; Sun, L.; Kloo, L.; Pettersson, H. *Chem. Rev.* **2010**, *110*, 6595−6663.

(2) Shockley, W.; Queisser, H. J. *J. Appl. Phys.* **1961**, *32*, 510−519.

(3) (a) Islam, A.; Chowdhury, F. A.; Chiba, Y.; Komiya, R.; Fuke, N.; Ikeda, N.; Nozaki, K.; Han, L. *Chem. Mater.* **2006**, *18*, 5178−5185. (b) Tian, H.; Yang, X.; Chen, R.; Hagfeldt, A.; Sun, L. *Energy Environ. Sci.* **2009**, *2*, 674−677. (c) Onozawa-Komatsuzaki, N.; Yanagida, M.; Funaki, T.; Kasuga, K.; Sayama, K.; Sugihara, H. *Inorg. Chem. Commun.* **2009**, *12*, 1212−1215.

(4) Péchy, P.; Renouard, T.; Zakeeruddin, S. M.; Humphry-Baker, R.; Comte, P.; Liska, P.; Cevey, L.; Costa, E.; Shklover, V.; Spiccia, L.; Deacon, G. B.; Bignozzi, C. A.; Grätzel, M. *J. Am. Chem. Soc.* **2001**, *123*, 1613−1624.

(5) (a) Robson, K. C. D.; Koivisto, B. D.; Yella, A.; Sporinova, B.; Nazeeruddin, M. K.; Baumgartner, T.; Grätzel, M.; Berlinguette, C. P. *Inorg. Chem.* **2011**, *50*, 5494−5508. (b) Kim, J. J.; Choi, H.; Paek, S.; Kim, C.; Lim, K.; Ju, M. J.; Kang, H. S.; Kang, M. S.; Ko, J. *Inorg. Chem.* **2011**, *50*, 11340−11347. (c) Funaki, T.; Funakoshi, H.; Kitao, O.; Onozawa-Komatsuzaki, N.; Kasuga, K.; Sayama, K.; Sugihara, H. *Angew. Chem., Int. Ed.* **2012**, *51*, 7528−7531.

(6) (a) Chen, B. S.; Chen, K.; Hong, Y. H.; Liu, W. H.; Li, T. H.; Lai, C. H.; Chou, P. T.; Chi, Y.; Lee, G. H. *Chem. Commun.* **2009**, 5844−5846. (b) Chou, C. C.; Wu, K. L.; Chi, Y.; Hu, W. P.; Yu, S. J.; Lee, G. H.; Lin, C. L.; Chou, P. T. *Angew. Chem., Int. Ed.* **2011**, *50*, 2054−2058. (c) Funaki, T.; Kusama, H.; Onozawa-Komatsuzaki, N.; Kasuga, K.; Sayama, K.; Sugihara, H. *Eur. J. Inorg. Chem.* **2014**, 1303−1311.

(7) (a) Li, G.; Ray, L.; Glass, E. N.; Kovnir, K.; Khoroshutin, A.; Gorelsky, S. I.; Shatruk, M. *Inorg. Chem.* **2012**, *51*, , 1614−1624. (b) Li, G.; Bomben, P. G.; Robson, K. C. D.; Gorelsky, S. I.; Berlinguette, C. P.; Shatruk, M. *Chem. Commun.* **2012**, *48*, 8790−8792.

(8) Smalley, S. J.; Waterland, M. R.; Telfer, S. G. *Inorg. Chem.* **2009**, *48*, 13−15.

(9) Li, G.; Hu, K.; Yi, C.; Knappenberger, K.; Meyer, G. J.; Gorelsky, S. I.; Shatruk, M. *J. Phys. Chem. C* **2013**, *117*, 17399−17411.

(10) (a) Nazeeruddin, M. K.; De Angelis, F.; Fantacci, S.; Selloni, A.; Viscardi, G.; Liska, P.; Ito, S.; Takeru, B.; Grätzel, M. *J. Am. Chem. Soc.* **2005**, *127*, 16835−16847. (b) Cao, Y.; Bai, Y.; Yu, Q.; Cheng, Y.; Liu, S.; Shi, D.; Gao, F.; Wang, P. *J. Phys. Chem. C* **2009**, *113*, 6290−6297.

(11) Ardo, S.; Meyer, G. J. *Chem. Soc. Rev.* **2009**, *38*, 115−164.

(12) Boschloo, G.; Gibson, E. A.; Hagfeldt, A. *J. Phys. Chem. Lett.* **2011**, *2*, 3016−3020.

(13) (a) Erten-Ela, S.; Yilmaz, M. D.; Icli, B.; Dede, Y.; Icli, S.; Akkaya, E. U. *Org. Lett.* **2008**, *10*, 3299−3302. (b) Kolemen, S.; Bozdemir, O. A.; Cakmak, Y.; Barin, G.; Erten-Ela, S.; Marszalek, M.; Yum, J. H.; Zakeeruddin, S. M.; Nazeeruddin, M. K.; Grätzel, M.; Akkaya, E. U. *Chem. Sci.* **2011**, *2*, 949−954.

5419

dx.doi.org/10.1021/ic5006538 | *Inorg. Chem.* 2014, 53, 5417−5419